Preprint Title	Heat-induced morphological changes in silver nanowires deposited on a patterned silicon substrate
Authors	Elyad Damerchi, Sven Oras, Edgars Butanovs, Allar Liivlaid, Mikk Antsov, Boris Polyakov, Annamarija Trausa, Veronika Zadin, Andreas Kyritsakis, Loïc Vidal, Karine Mougin, Siim Pikker and Sergei Vlassov
Publication Date	24 Jan. 2024
Article Type	Full Research Paper
Supporting Information File 1	Supplementary Information.docx; 30.1 MB
ORCID® iDs	Edgars Butanovs - https://orcid.org/0000-0003-3796-1190; Mikk Antsov - https://orcid.org/0000-0003-1291-3520; Annamarija Trausa - https://orcid.org/0000-0001-9298-9490; Siim Pikker - https://orcid.org/0000-0003-2260-7594; Sergei Vlassov - https://orcid.org/0000-0001-9396-4252

Heat-induced morphological changes in silver nanowires deposited on a patterned silicon substrate

Elyad Damerchi[1], Sven Oras[1], Edgars Butanovs[1,2], Allar Liivlaid[1], Mikk Antsov[3], Boris Polyakov[2], Annamarija Trausa[2], Veronika Zadin[1], Andreas Kyritsakis[1], Loïc Vidal[4], Karine Mougin[4], Siim Pikker[5], Sergei Vlassov[5]

[1]*Institute of Technology, University of Tartu, Nooruse 1, 50411 Tartu, Estonia*

[2]*Institute of Solid State Physics, University of Latvia, Kengaraga 8, LV-1063 Riga, Latvia*

[3]*Estonian Military Academy, Riia 12, 51010 Tartu, Estonia*

[4]*Institute of Materials Science of Mulhouse, CNRS – UMR 7361, University of Haute-Alsace, France*

[5]*Institute of Physics, University of Tartu, W. Ostwaldi 1, 50411 Tartu, Estonia*

Abstract

Metallic nanowires (NWs) are sensitive to heat treatment and can split into shorter fragments within minutes at temperatures far below the melting point. This process can hinder the functioning of NW-based devices that are subject even to relatively mild temperatures. Commonly, heat-induced fragmentation of NWs is attributed to the interplay between heat-enhanced diffusion and Rayleigh instability. In this work we demonstrated that contact with the substrate plays an important role in the fragmentation process and can strongly affect the outcome of the heat treatment. We deposited silver NWs onto specially patterned silicon wafers so that some NWs were partially suspended over the holes in the substrate. Then we performed a series of heat-treatment experiments and found that adhered and suspended parts of NWs behave differently under the heat-treatment. Moreover, depending on the heat-treatment process, fragmentation in either adhered or suspended parts can dominate. Experiments were supported by finite element method and molecular dynamics simulations.

Keywords

silver nanowires, heat treatment, scanning electron microscopy, morphological changes, diffusion.

1 Introduction

Metal nanowires (NWs) are promising key elements in wide range of applications including solar cells[1], smart windows[2], flexible sensors[3], touch screens[4], biocompatible polymer binders[5], temperature sensing [6], medical materials[7], key elements of nanoscale devices[8], and other. When deposited on a transparent substrate in the form of a low-density mesh, metal NWs can provide

electrical conductivity while retaining sufficient transparency. The growing demand for transparent conductive materials has stimulated numerous studies aimed at the design, preparation, and characterization of such materials[9,10]. One of the most studied materials for NW-based transparent electrodes is silver (Ag). Ag NWs of high quality can be relatively easily synthesized in large amounts with a high degree of control over the length and diameter [11,12]. In comparison to indium tin oxide (ITO), which currently is the industry standard in transparent conductive films, the Ag NW network is mechanically much more flexible and provides a significantly wider optical transmittance range that spreads far beyond the visible region [13,14]. Another related application for Ag NW networks is highly flexible transparent film heaters [15]. In recent years Ag NWs attracted attention as a key element of neuromorphic computing devices.[16]

In the aforementioned applications, Ag NWs are subjected to elevated temperatures caused by Joule heating. [17] Moreover, heat treatment at a few hundred degrees Celsius is often used after the deposition of NWs onto the substrate to burn out the surfactant used in the synthesis. [18,19] The melting temperature of silver is 962 °C, which is significantly higher than the temperatures required to remove organics. However, it is well known that the behavior of metal nanostructures under elevated temperatures can differ drastically compared to their bulk counterparts being not only material- but also size- and shape-dependent [20,21]. In general, metal nanostructures melt at lower temperatures compared to the bulk, and the melting temperature decreases with reduction of the size and dimensionality (nanoparticles in general have lower melting temperature than NWs of the same diameter) of the structures [20,22,23]. This phenomenon is generally related to variation of surface energy with size [24]. The decrease of melting temperature can reach a few hundred degrees for sizes below 10 nm. [25] The diameters of Ag NWs used in real applications are typically larger. However, in case of a prolonged heat treatment (minutes and above) heat-enhanced diffusion of surface atoms can result in morphological changes in NWs at temperatures many hundreds degrees below the melting point of the material [26,27]. Sintering of Ag and Au NWs at intersections can happen at temperatures as low as 125 – 200 °C within minutes.[27,28] This effect is beneficial for increasing electrical conductivity of a NW network by improving electrical contacts between individual NWs. [28–30] However, a further increase in temperature can result in the splitting of NWs into shorter fragments driven by Rayleigh instability and energy minimization via spheroidization [28,31]. The kinetics of diffusive processes in NWs are tightly related to surface energies of the system. Both Ag and Au NWs have pentagonal cross-section meaning that for NWs deposited on a flat substrate 1/5 of the NW surface is in contact with the substrate [32]. This aspect unavoidably should have an influence on total surface energy of NW. Therefore, in addition to parameters like temperature, time, and geometry of NWs, contact with the substrate can potentially have a considerable effect on heat-induced changes in NWs. Understanding of metal NW fragmentation behavior under different conditions and on various substrates could improve a degree of control in a cost-effective production methods in various novel applications where arrays of metal nanostructures are used, such as e.g. surface-enhanced Raman spectroscopy substrates [33–35].

In this work, we deposited Ag NWs on a specially patterned silicon (Si) substrate so that large fractions of NWs are partially suspended over the holes. Samples then were heated to different temperatures in air and the behavior of suspended versus adhered part under heating is compared. Experiments are supplemented with molecular dynamics (MD) and finite element method (FEM) simulations.

2 Materials and methods

2.1 Preparation of samples

Ag NWs with a nominal diameter of 120 nm and length in tens of micrometers were purchased from Blue Nano, Inc. These NWs have pentagonal cross-section and five-fold twinned inner structure. More details on the structure and properties of these NWs can be found in our previous works [32,36].

The patterned silicon substrates with square holes were prepared from (100) silicon wafers (Semiconductor wafer, Inc.) with 50 nm thermal oxide in four steps as follows: 1) conventional optical lithography process to produce the desired pattern in a photoresist on the wafer; 2) selective removal of SiO_2 using buffered HF solution in order to replicate the resist pattern in the oxide layer; 3) silicon etching in tetramethylammonium hydroxide (TMAH) solution at 90°C to create the etch pits; 4) rinse in HF to remove the remaining SiO_2. Resulting substrates had rectangular holes with the side length in the order of few μm (3.6 to 5.3 μm) and depth in order of several hundreds of nm. The distance between holes depending on direction varied from hundreds of nm to several μm. The slope of the sidewalls of the holes relative to the main surface of the silicon is 54.7 degrees that corresponds to the angle between (111) and (001) planes in Si.

Samples for heat-treatment studies were prepared by drop-casting the Ag NWs onto the patterned substrates from a solution. Since the width and period of the holes were intentionally made much smaller than the average length of NWs, many NWs crossed several holes simultaneously. Such configuration is highly beneficial as it enables to study the effect of the substrate on the same NW by comparing the behavior of suspended versus adhered parts (Figure 1).

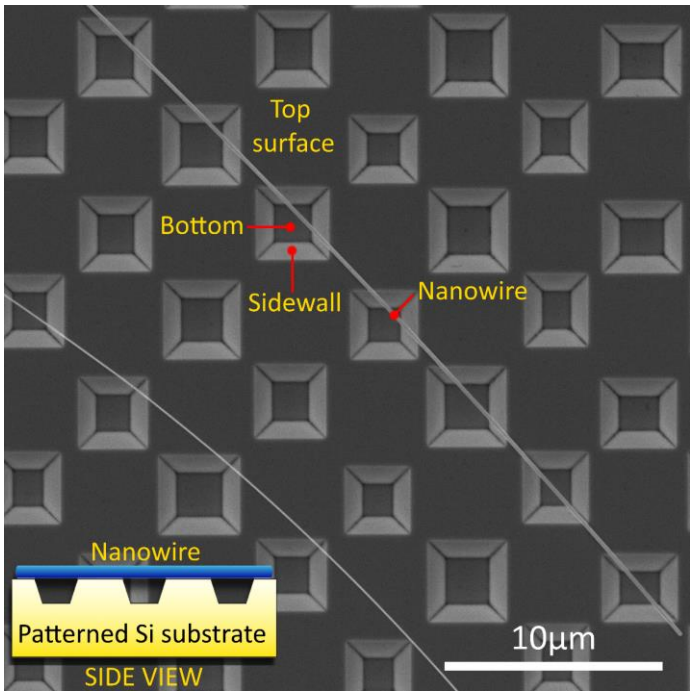

Figure 1. Single Ag NW suspended over several holes etched in Si substrate.

2.2 Heat treatment and characterization

Heat-treatment experiments were carried out in a muffle furnace (NABERTHERM, L-091H1RN-240). Samples were placed into the furnace that was already pre-heated to the target temperature and were removed after 10 minutes from the hot furnace and were naturally cooled in air at room temperature. Heating time (10 minutes) was chosen to have comparability with the work by Vigonski et al [27] who used the same Ag NWs and heating methods for heat-treatment experiments of a flat Si substrate.

Two heating schemes were implemented:

- In the scheme 1 (Figure 2), heating was applied in 10-minute cycles at fixed temperatures followed by cooling to room temperature. The temperature of the first cycle was 100 °C and in each following step, it was increased by 50 °C until 200 °C, and then by 25 °C increments until reaching 450 °C.
- In the scheme 2 (Figure 2), freshly made samples were heated in a single step for 10 minutes at a target temperature chosen based on the results from the scheme 1.

SEM (FEI, Nanosem 450) images were collected before and after each heating cycle.

Additionally, a separate series of experiments were performed in TEM to study the effect of heat treatment on the inner structure of NWs. Two TEMs (TEM, Tecnai GF20, FEI and JEOL microscope, model ARM-200F) were used operated at 200 kV accelerating voltage.

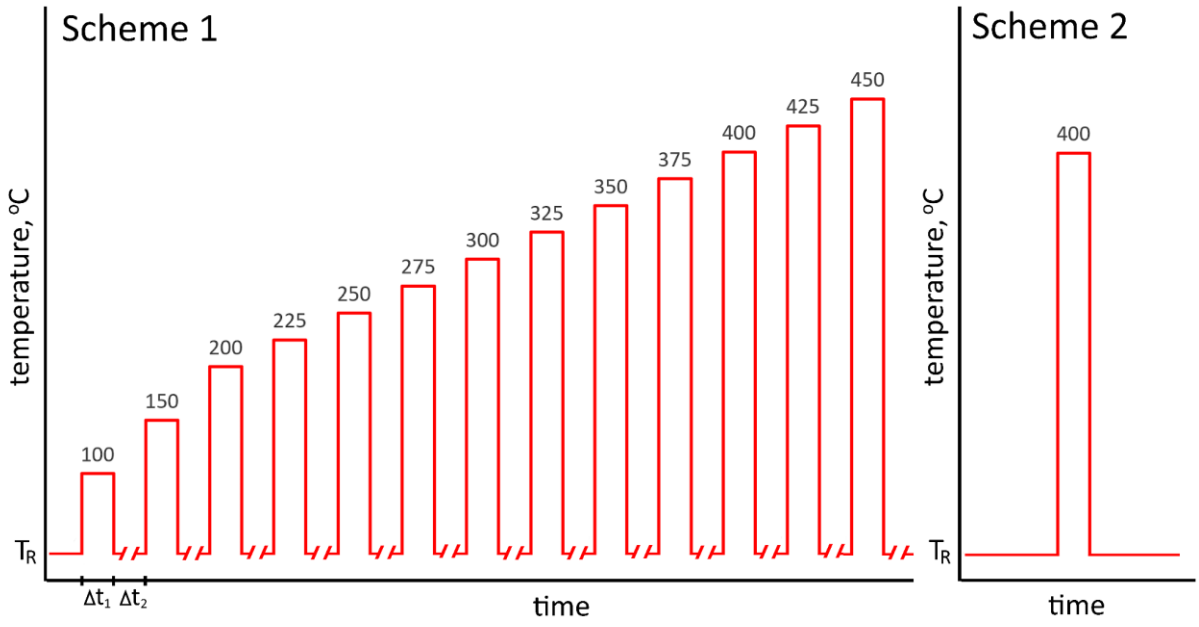

Figure 2. Heating schemes used for heat treatment of Ag NWs. T_R stands for room temperature. Δt_1 = 10 min is a heat treatment time, $\Delta t_2 \approx 1$ h is the rest time.

2.3 Simulations

The extent and distribution of mechanical stresses induced by thermal expansion of Ag NW and a substrate during heat treatment from room temperature to 673.15 K were simulated by FEM in Comsol Multiphysics 5.6. The structural configuration involved a pentagonal Ag NW positioned above a rectangular hole on an Si substrate. The NW was securely affixed to the substrate, while the overhanging segment retained freedom of movement in all directions. The elastic modulus values for the Ag NW and Si substrate were set to the built-in values in Comsol, accounting for their temperature-dependent nature. More technical details can be found in SI.

MD simulations were performed with the Large-scale Atomic/Molecular Massively Parallel Simulator (LAMMPS)[37]. Interactions between the atoms were governed by the embedded atom method (EAM) potential [38] for silver atoms. Visualization was performed with the Open Visualization Tool (OVITO) [39]. The system timestep was 10 fs. More technical details can be found in SI.

3 Results and discussion

3.1 Heat-treatment

3.1.1 First heating scheme

No significant changes in the morphology of Ag NWs were detected for heat-treatment temperatures up to 275 °C. Starting from 300 °C, the first clear signs of diffusion in NWs appeared in the form of splitting at the places where NWs were partly broken during deposition (Figure 3). In addition, fusion at the intersections of two or more NWs (Figure S1) was observed, in agreement with other studies[27,28,30,40]. No difference in behavior between adhered and suspended parts of NWs regarding structural integrity was detected by this point. The only noticeable factor influencing the process was the diameter of NWs: in general, thinner NWs started to diffuse earlier.

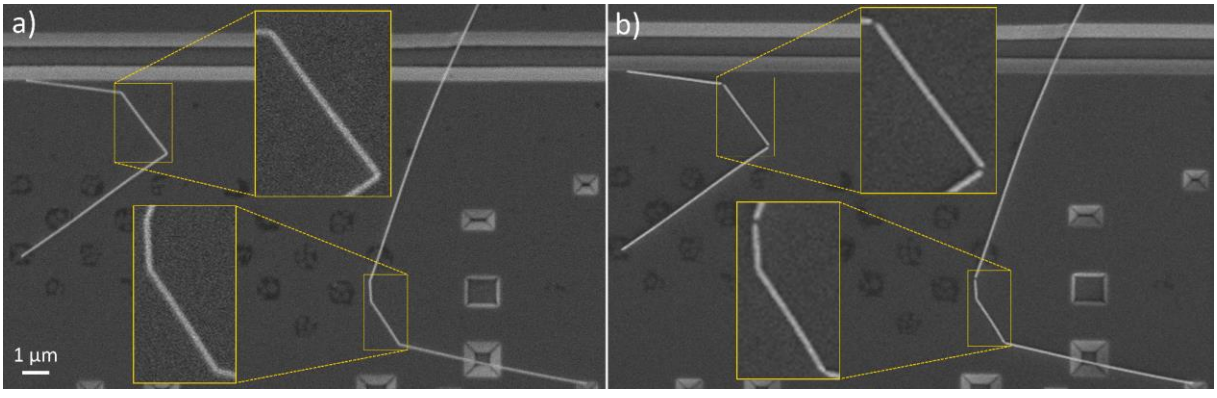

Figure 3. a) Ag NWs deformed after deposition onto Si substrate. b) Splitting of the Ag NWs at the bending areas after 4 heating cycles (100, 150, 200, and 225 °C) in scheme 1.

In the temperature range from 350 °C to 375 °C, necking and complete splitting of Ag NWs approximately in the middle of suspended parts (Figure 4) was observed in many NWs. Starting from 400 °C fragmentation of NWs spread to the adhered parts (Figure S2). From this finding,

it can be concluded that in the heating scheme 1, adhered parts are more heat-resistant and can withstand approximately 50 °C higher temperatures before fragmentation compared to the suspended parts. By 450 °C most NWs were split in the suspended parts, and extensive fragmentation was present also in the adhered parts. Again, in general, thinner NWs were more prone to necking and splitting, while thicker NWs withstood higher temperatures.

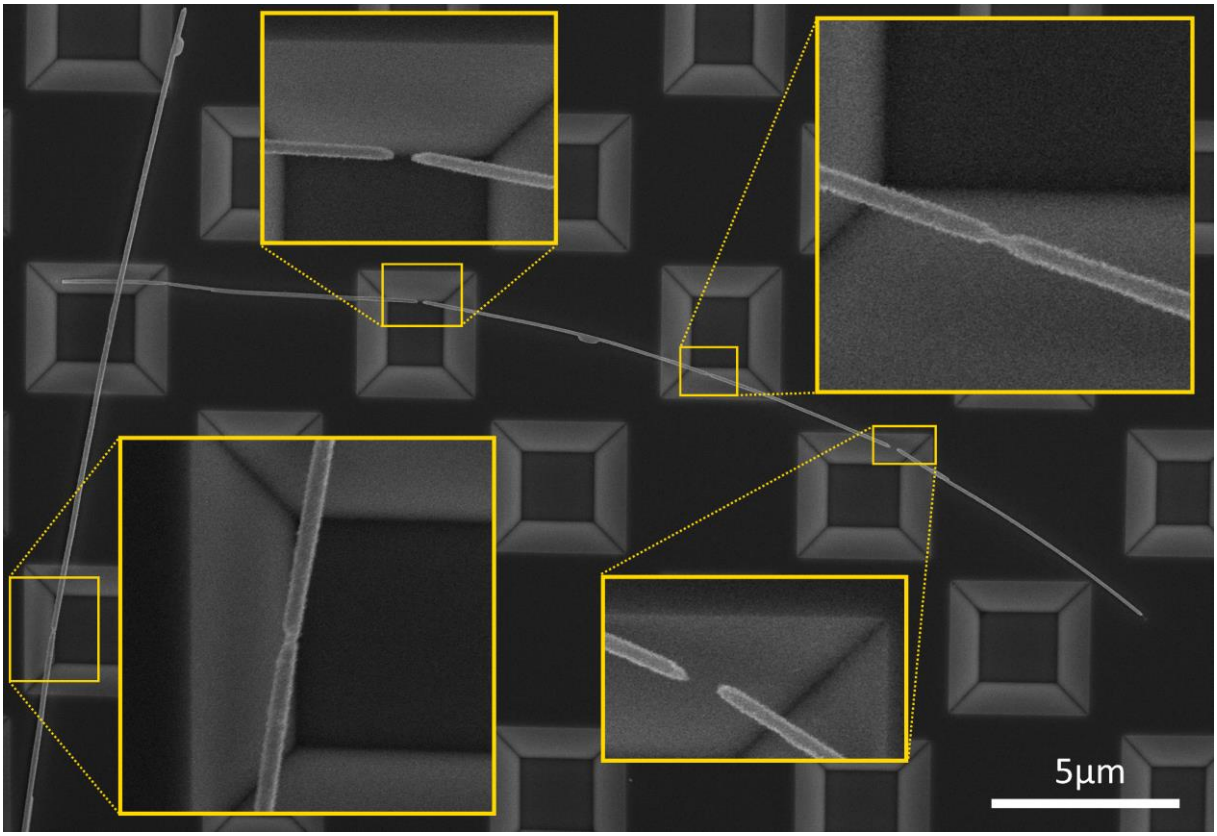

Figure 4. Necking and splitting of Ag NWs in the first heating scheme after treatment at 375 C.

3.1.2 Second heating scheme

For scheme 2, it was possible to "catch" the early stage of fragmentation of NWs, which is essential for comparison of the behavior of adhered and suspended parts under heat-treatment, in the temperature range of 375 - 400°C. It was found that the behavior of partially suspended NWs in the heating scheme 2 was completely opposite to what we found in the heating scheme 1. Namely, extensive fragmentation occurred in the adhered parts while the suspended parts remained in one piece (Figure 5). The effect was most pronounced for the samples treated at 400°C. Above that temperature extensive fragmentation was observed in both adhered and suspended parts.

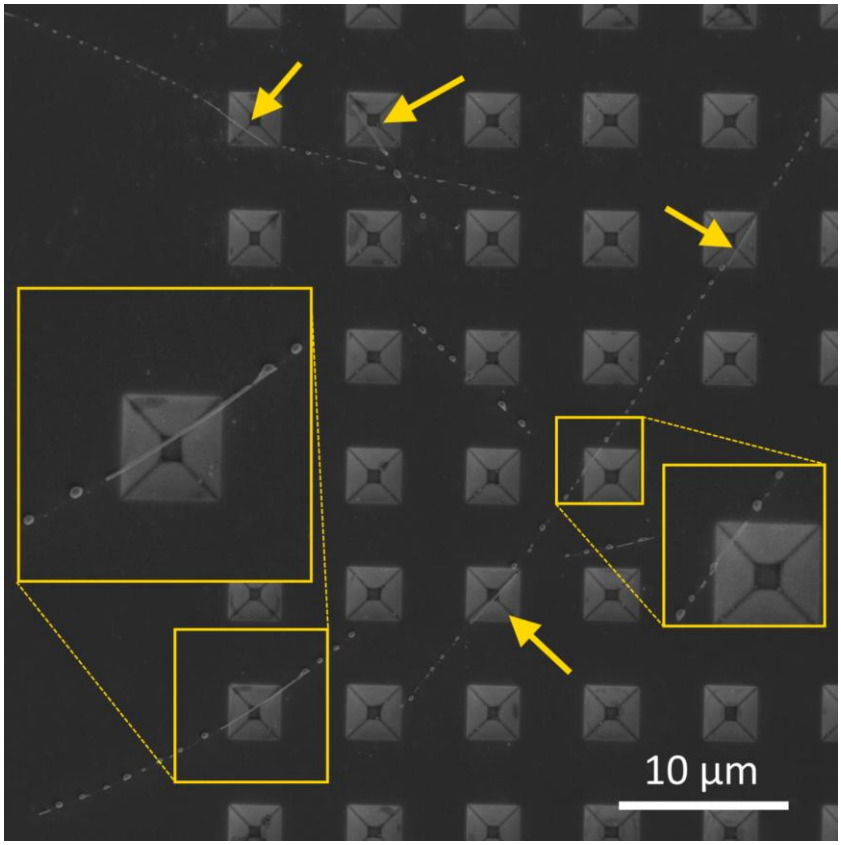

Figure 5. SEM images of Ag NWs after a single-step heat treatment (second heating scheme) at 400°C. Fragmentation of NWs happened almost exclusively in the adhered parts.

The heat-treatment experiments (both heating schemes) were repeated two times, each time on freshly made samples and following the same protocol of the heating scheme. Each time the results consistently demonstrated the tendency to split first in the middle of the suspended part for the heating scheme 1, and in the adhered part for the heating scheme 2.

To quantitatively describe the extent of splitting in the adhered and suspended parts of Ag NWs, we introduced two parameters: “splits per part”, which denotes the total number of split events separately for the adhered and suspended parts of each NW, and “splits per unit length”, which indicate the number of split events per length of either adhered or suspended part. Then, the average values for all analyzed NWs were calculated separately for each heating scheme. In total, 111 adhered and 101 suspended parts were analyzed for the heating scheme 1, and 87 adhered and 64 suspended parts for the heating scheme 2. Normalized results of the statistical analysis are given in Figure 6. For the heating scheme 1 the extent of fragmentation in the suspended parts is one order of magnitude higher than that for the adhered parts, while totally opposite behavior is observed for the heating scheme 2.

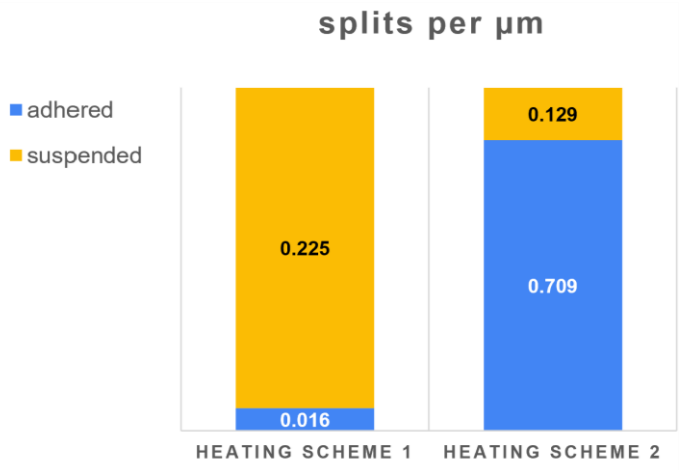

Figure 6. Average values of splits per length unit in adhered and suspended parts for both heating schemes.

3.2 Inner structure of Ag nanowires

Ag NWs used in the present study have a five-fold twinned crystal structure resulting in a pentagonal cross-section. Since pentagonal symmetry is a "forbidden" symmetry in crystallography, five-fold twinned crystals unavoidably have inner strains [41]. This potentially could be one of the driving forces leading to heat-induced fragmentation of Ag NWs as the mechanism of stress release and could potentially involve recrystallization into single crystals. To test this hypothesis, we repeated experiments on TEM grids with subsequent observation of crystal structure in TEM. It was found that the pentagonal structure is preserved even for small fragments of NWs that were split as a result of heat-treatment as shown in Figure 7 (note that fragments are kept in place due to contact with the thin carbon membrane of the TEM grid). This finding suggests that heat-induced morphological changes in Ag NWs occur via surface diffusion without the loss of crystal structure.

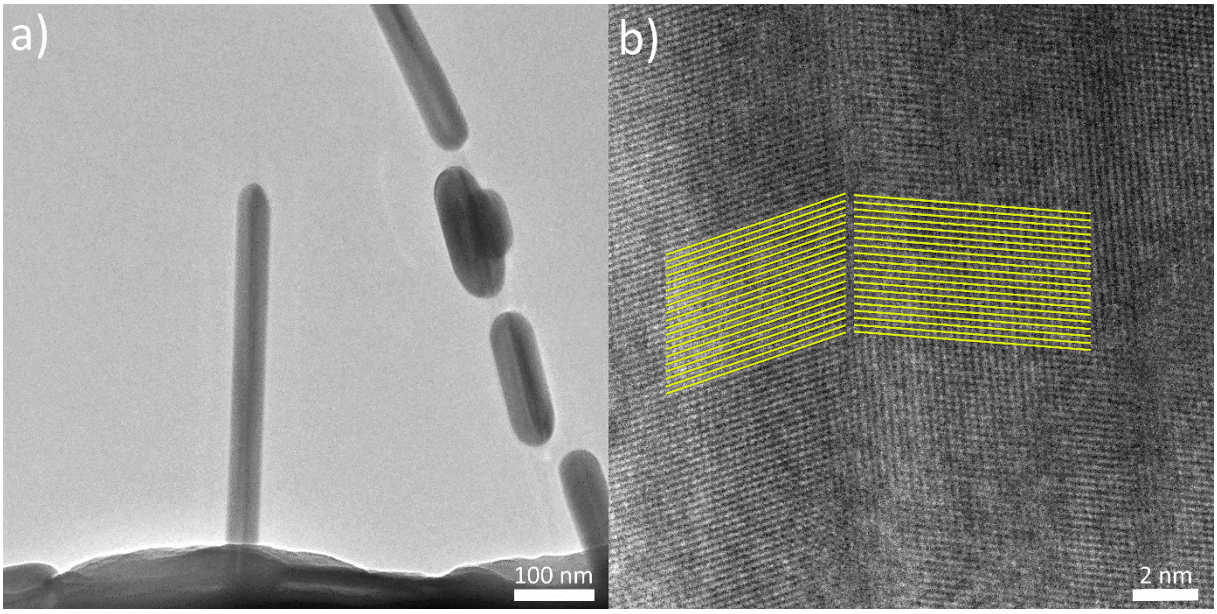

Figure 7. TEM images of Ag NWs after single-step (scheme 2) heat-treatment. Dark lines in the middle of NWs correspond to a twin-border between two crystal segments.

3.3 Hypothesis and simulations

According to our understanding, there are several key aspects that should be considered in order to explain the results of the heat-treatment experiments.

- Ag has almost an order of magnitude higher thermal expansion coefficient compared to Si (18.9 vs $2.8*10^{-6}$ m/(mC°))[42].
- From nanomanipulation experiments previously performed on similar Ag NWs[8], we know that the strength of the contact between Ag NWs and Si substrate can exceed the ultimate strength of Ag NWs.

Based on these facts, we expect that the thermal expansion of Ag NWs will compete with friction forces between NW and Si substrate, causing significant mechanical stresses inside NWs, especially at the interface between the two materials. This may serve as a driving force for the redistribution of Ag atoms and splitting of the adhered part of a NW into shorter fragments as a mechanism for stress mitigation. For the suspended parts the thermal expansion should result in deformation. To estimate the extent and distribution of the heat-induced mechanical stresses in a partially suspended NW, we performed corresponding FEM simulations (Figure S3). According to simulations, the highest stresses (up to 1.5×10^9 N/m^2) are concentrated at the interface between the adhered part and Si substrate, followed by the stresses in the middle of the suspended part (up to 1×10^9 N/m^2).

In this simplified idealistic model, the contact between a NW and Si is absolutely rigid, preventing any slippage or plastic deformation at the interface. Moreover, FEM simulations do not include possible rearrangement of atoms that can occur in the real system as a mechanism of stress mitigation. The model is completely elastic and the simulated processes are fully reversible. Therefore, the results of FEM simulations should be treated only as a simplified qualitative illustration of the thermomechanical processes that may occur in the real system. Nevertheless, such results may give an additional hint for understanding the mechanisms responsible for splitting in different configurations.

In particular, we can speculate that repeated heat-induced bending of the suspended part in Scheme 1 can lead to fatigue and formation of defects in the middle of the suspended part. This effect should be even more pronounced if we assume that a NW is deformed and stressed only in the early stage of the hot phase following by a gradual relaxation of the NW by the means of heat-enhanced rearrangement of silver atoms at the contact with the substrate as a mechanism of stress mitigation. In other words, the NW will "slide" along the substrate to adapt for heat-induced elongation without deformation. When the sample is removed from the hot furnace, rapid cooling and thermal contraction should give rise to tensile stresses inside the NW, especially considering the greatly reduced mobility of Ag atoms at lower temperatures preventing slippage of NW relative to Si substrate. As a result, defects and necking will develop in the middle of the suspended part, which agrees with the experimentally observed necking in Scheme 1 (Figure 4). As was shown above (Figure 3), heat-induced splitting tends to occur first at regions that have significant structural defects, which is also discussed in more detail by Mayoral et al., [43], and Sun et al[44]. According to the latter, atoms in a NW tend to diffuse away from the regions of critical defects. Diffusion is expected to start mainly at the surface resulting in the thinning of the NW in the middle of the suspended part. It means that a further heat treatment will result in the splitting of the necking region before the NW splits anywhere else.

Therefore, we have a potential mechanism responsible for splitting of NW in the suspended part in Scheme 1. The process is schematically shown in the Figure 8 - Scheme 1.

For Scheme 2 the situation is simpler. Since there are no heating cycles involved, the suspended parts do not experience repeated compression and tensile stresses. The adhered parts split into shorter fragments similar way it generally happens with heated Ag and Au NWs on a flat silicon substrate[27]. This process is commonly explained by the phenomena known as Reyleigh instability[45–47]. According to our understanding, stresses which arise at the interface between the NW and the substrate due to the difference in thermal expansion, also play a crucial role in the process. Thus, fragmentation of NWs can be attributed to the interplay between heat-induced mechanical stresses and Rayleigh instability. Otherwise, the fragmentation would be similar regardless of the contact with the substrate. In the experiments, however, the suspended parts survive longer as they avoid interfacial stresses. Note that in some cases the length of the survived part is longer than the length of the suspended part. A possible reason is that the heat-induced bending can cause the detachment of the NW close to the hole similar to peeling or crack formation and propagation. The process is schematically shown in the Figure 8 - Scheme 2.

Note that, as mentioned earlier, the evolution of morphology in the adhered parts is similar for both schemes. Namely, fragmentation of adhered parts into shorter particles at higher temperature will be observed in both cases. Main differences are observed in suspended parts at transitional temperatures when the first morphological changes in individual NWs are clearly visible.

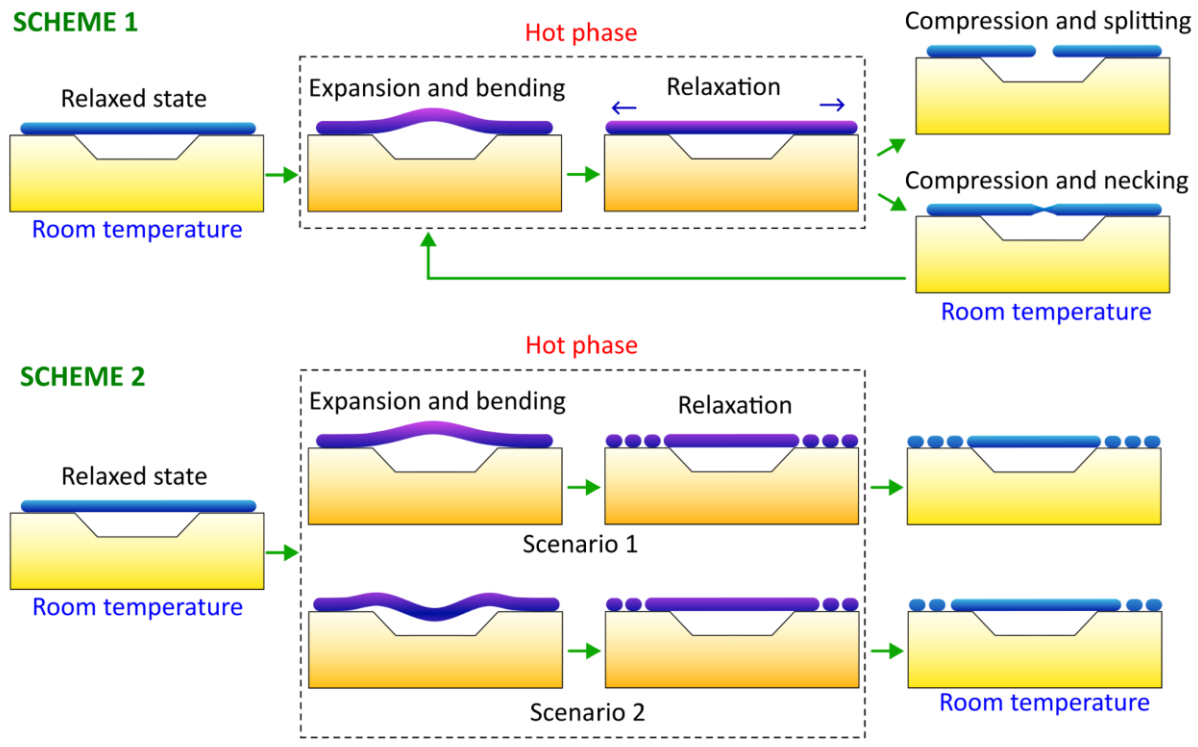

Figure 8. Schematic representation of the deformation and fragmentation of NWs during the heat-treatment.

To further investigate the role of stress-induced defects in the splitting of NWs at elevated temperatures in Scheme 1, we performed MD simulations (see detailed description in SI). A NW was simulated as a periodic prismatic rod with pentagonal cross-section and five-fold twinned inner structure (Figure 9). A series of heating and cooling cycles were applied, accompanied by compression and tensile deformations along the NW. The heating cycling induced formation of defects and amorphous regions being the most pronounced in the central part of the NW with subsequent evolution into necking and finally splitting (Figure 9b-c).

It should be noted that the goal of the MD simulations was only to qualitatively evaluate the role of the thermomechanically induced defects in fragmentation of five-fold twinned Ag NWs. Therefore, the model has significant differences and simplifications compared to the real experiment. Namely, an isolated NW was simulated, which excludes the role of the substrate in the process. The diameter of the NW model was an order of magnitude smaller compared to the experiment. To compensate for the drastic difference in the timescales between the experiment (minutes) and simulations (nanoseconds), significantly higher (but still below melting point) temperatures were used in the simulations. Nevertheless, MD results qualitatively agree well with the TEM images of the NWs which underwent several heating-cooling cycles (Figure 9d).

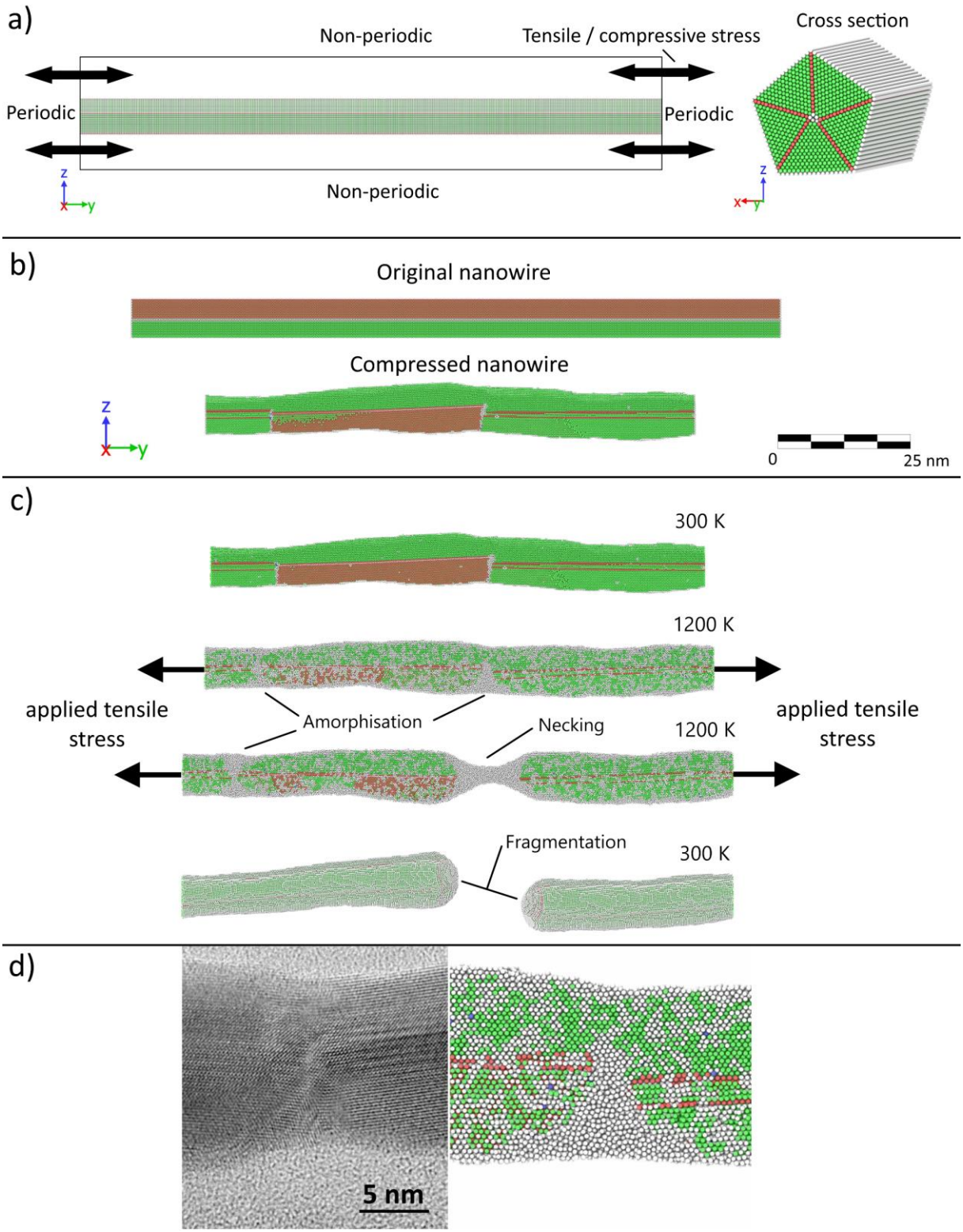

Figure 9. MD model of the NW: (a) initial conditions, (b) results of the compression cycle, (c) results of the tensile deformation; (d) amorphization of the central part of the NW as a result of heat-treatment cycles: TEM image (left) and MD simulation frame taken when the structure had turned amorphous but not yet broken (right). Color code: Green - FCC lattice, Red – HCP, Blue – BCC, White – amorphous.

3.4 Other heat-induced effect

In addition to the above-mentioned effects, it was found that in both schemes the heat-treatment sometimes caused residual elongation and bending of the suspended parts. One example is given in Figure S4 showing a significant bending in the suspended part in the heating scheme 2. The onset temperature of this phenomenon is difficult to determine as the deformation can be below the detection limits of SEM. Moreover, in SEM we only see 2D projection normal to the electron beam. If NWs are bent out of the substrate plane (upwards or downwards) it will not be visible in the SEM image.

If a NW is contacting one or more other NWs, then heat-induced redistribution of silver atoms between NWs is often observed resulting in thickening and shortening of all the contacting NWs (Figure S5). Some NWs may completely disappear in this process, being absorbed by the neighbors, as described also by Mayoral et. al[43]. In this work we focused on the individual NWs, therefore detailed analysis of the NW bundles lies outside the scope of the present study.

4 Conclusions

In this work, we investigated the effect of heat-treatment on pentagonal Ag nanowires that are only partially in contact with the substrate. We deposited Ag nanowires on patterned Si substrates which had arrays of holes of different sizes so that some nanowires were partially suspended over the holes. We found that if the temperature is increased in stepwise (in 25 °C increments) cycles of rapid heating followed by rapid cooling to room temperature after each cycle (scheme 1), then at 375 °C, nanowires start to split in the middle of the suspended parts, while the adhered parts remain mostly intact (0.225 vs 0.016 splits per µm). If the temperature is increased directly from room temperature to 375 °C or 400 °C (scheme 2), the opposite behavior is observed. Namely, most suspended parts remain intact, while extensive fragmentation occurs in the adhered parts (0.129 vs 0.709 splits per µm). At temperatures above 400 °C both the adhered and suspended parts are involved in fragmentation. According to our understanding such behavior is related to mechanical stresses which arise in nanowires as interplay between thermal expansion and frictional forces. The finite element method and molecular dynamic simulations gave good qualitative agreement with the experimental observations.

Acknowledgements

The work was funded by ERA Chair MATTER from the European Union's Horizon 2020 research and innovation programme under grant agreement No 856705, and by European Regional Development Fund project Nr. 1.1.1.1/21/A/053 realized at the Institute of Solid State Physics, University of Latvia. Institute of Solid State Physics, University of Latvia as the Center of Excellence has received funding from the European Union's Horizon 2020 Framework Programme H2020-WIDESPREAD-01-2016-2017-TeamingPhase2 under grant agreement No. 739508, project CAMART2. Authors are grateful to Pakeeza Afzal for assistance.

5 References

(1) Langley, D. P.; Giusti, G.; Lagrange, M.; Collins, R.; Jiménez, C.; Bréchet, Y.; Bellet, D. Silver Nanowire Networks: Physical Properties and Potential Integration in Solar Cells. *Sol. Energy Mater. Sol. Cells* **2014**, *125*, 318–324. https://doi.org/10.1016/j.solmat.2013.09.015.

(2) Large Area Co-Assembly of Nanowires for Flexible Transparent Smart Windows. https://doi.org/10.1021/jacs.7b03227.

(3) Ke, S.; Guo, P.; Pang, C.; Tian, B.; Luo, C.; Zhu, H.; Wu, W. Screen-Printed Flexible Strain Sensors with Ag Nanowires for Intelligent and Tamper-Evident Packaging Applications. *Adv. Mater. Technol.* **2020**, *5* (5), 1901097. https://doi.org/10.1002/admt.201901097.

(4) Madaria, A. R.; Kumar, A.; Zhou, C. Large Scale, Highly Conductive and Patterned Transparent Films of Silver Nanowires on Arbitrary Substrates and Their Application in Touch Screens. *Nanotechnology* **2011**, *22* (24), 245201. https://doi.org/10.1088/0957-4484/22/24/245201.

(5) Jin, Y.; Deng, D.; Cheng, Y.; Kong, L.; Xiao, F. Annealing-Free and Strongly Adhesive Silver Nanowire Networks with Long-Term Reliability by Introduction of a Nonconductive and Biocompatible Polymer Binder. *Nanoscale* **2014**, *6* (9), 4812–4818. https://doi.org/10.1039/C3NR05820D.

(6) Yin, R.; Yang, S.; Li, Q.; Zhang, S.; Liu, H.; Han, J.; Liu, C.; Shen, C. Flexible Conductive Ag Nanowire/Cellulose Nanofibril Hybrid Nanopaper for Strain and Temperature Sensing Applications. *Sci. Bull.* **2020**, *65* (11), 899–908. https://doi.org/10.1016/j.scib.2020.02.020.

(7) Yamini, S.; Gunaseelan, M.; Kumar, G. A.; Singh, S.; Dannangoda, G. C.; Martirosyan, K. S.; Sardar, D. K.; Sivakumar, S.; Girigoswami, A.; Senthilselvan, J. NaGdF4:Yb,Er-Ag Nanowire Hybrid Nanocomposite for Multifunctional Upconversion Emission, Optical Imaging, MRI and CT Imaging Applications. *Microchim. Acta* **2020**, *187* (6), 317. https://doi.org/10.1007/s00604-020-04285-9.

(8) Vlassov, S.; Oras, S.; Antsov, M.; Butikova, J.; Lõhmus, R.; Polyakov, B. Low-Friction Nanojoint Prototype. *Nanotechnology* **2018**, *29* (19), 195707. https://doi.org/10.1088/1361-6528/aab163.

(9) Arefpour, M.; Almasi Kashi, M.; Khansari Barzoki, F.; Noormohammadi, M.; Ramazani, A. Electrodeposited Metal Nanowires as Transparent Conductive Electrodes: Their Release Conditions, Electrical Conductivity, Optical Transparency and Chemical Stability. *Mater. Des.* **2018**, *157*, 326–336. https://doi.org/10.1016/j.matdes.2018.07.048.

(10) Metal-Based Flexible Transparent Electrodes: Challenges and Recent Advances. https://doi.org/10.1002/aelm.202001121.

(11) Choi, J.; Sauer, G.; Nielsch, K.; Wehrspohn, R. B.; Gösele, U. Hexagonally Arranged Monodisperse Silver Nanowires with Adjustable Diameter and High Aspect Ratio. *Chem. Mater.* **2003**, *15* (3), 776–779. https://doi.org/10.1021/cm0208758.

(12) Nuriyeva, S. G.; Shirinova, H. A.; Hasanov, K. M.; Hajiyeva, F. V. Controlled Synthesis of Silver Nanowires: Production and Characterization. *Acta Phys. Pol. ISSN 1898-794X* **2023**, *143* (4), 279–279. https://doi.org/10.12693/APhysPolA.143.279.

(13) Langley, D.; Giusti, G.; Mayousse, C.; Celle, C.; Bellet, D.; Simonato, J.-P. Flexible Transparent Conductive Materials Based on Silver Nanowire Networks: A Review. *Nanotechnology* **2013**, *24* (45), 452001. https://doi.org/10.1088/0957-4484/24/45/452001.

(14) Bardet, L.; Papanastasiou, D. T.; Crivello, C.; Akbari, M.; Resende, J.; Sekkat, A.; Sanchez-Velasquez, C.; Rapenne, L.; Jiménez, C.; Muñoz-Rojas, D.; Denneulin, A.; Bellet, D. Silver Nanowire Networks: Ways to Enhance Their Physical Properties and Stability. *Nanomaterials* **2021**, *11* (11), 2785. https://doi.org/10.3390/nano11112785.
(15) Celle, C.; Mayousse, C.; Moreau, E.; Basti, H.; Carella, A.; Simonato, J.-P. Highly Flexible Transparent Film Heaters Based on Random Networks of Silver Nanowires. *Nano Res.* **2012**, *5* (6), 427–433. https://doi.org/10.1007/s12274-012-0225-2.
(16) Diaz-Alvarez, A.; Higuchi, R.; Sanz-Leon, P.; Marcus, I.; Shingaya, Y.; Stieg, A. Z.; Gimzewski, J. K.; Kuncic, Z.; Nakayama, T. Emergent Dynamics of Neuromorphic Nanowire Networks. *Sci. Rep.* **2019**, *9* (1), 14920. https://doi.org/10.1038/s41598-019-51330-6.
(17) Khaligh, H. H.; Goldthorpe, I. A. Failure of Silver Nanowire Transparent Electrodes under Current Flow. *Nanoscale Res. Lett.* **2013**, *8* (1), 235. https://doi.org/10.1186/1556-276X-8-235.
(18) Chen, S.; Guan, Y.; Li, Y.; Yan, X.; Ni, H.; Li, L. A Water-Based Silver Nanowire Ink for Large-Scale Flexible Transparent Conductive Films and Touch Screens. *J. Mater. Chem. C* **2017**, *5* (9), 2404–2414. https://doi.org/10.1039/C6TC05000J.
(19) Shi, Y.; He, L.; Deng, Q.; Liu, Q.; Li, L.; Wang, W.; Xin, Z.; Liu, R. Synthesis and Applications of Silver Nanowires for Transparent Conductive Films. *Micromachines* **2019**, *10* (5), 330. https://doi.org/10.3390/mi10050330.
(20) Guisbiers, G. Advances in Thermodynamic Modelling of Nanoparticles. *Adv. Phys. X* **2019**, *4* (1), 1668299. https://doi.org/10.1080/23746149.2019.1668299.
(21) Jabbareh, M. A. A Unified Bond Energy Model for Size-Dependent Melting Temperature of Freestanding and Embedded Nanomaterials. *Solid State Commun.* **2022**, *355*, 114923. https://doi.org/10.1016/j.ssc.2022.114923.
(22) Shuai, Z. The Dimensional Dependence of the Shape Factor on Thermodynamics. *Nanomater. Energy* **2020**, *9* (2), 234–237. https://doi.org/10.1680/jnaen.19.00039.
(23) Fu, Q.; Cui, Z.; Xue, Y.; Duan, H. Research of Size- and Shape-Dependent Thermodynamic Properties of the Actual Melting Process of Nanoparticles. *J. Phys. Chem. C* **2018**, *122* (27), 15713–15722. https://doi.org/10.1021/acs.jpcc.8b03085.
(24) Ouyang, G.; Li, X. L.; Tan, X.; Yang, G. W. Surface Energy of Nanowires. *Nanotechnology* **2008**, *19* (4), 045709. https://doi.org/10.1088/0957-4484/19/04/045709.
(25) Schmid, G.; Corain, B. Nanoparticulated Gold: Syntheses, Structures, Electronics, and Reactivities. *Eur. J. Inorg. Chem.* **2003**, *2003* (17), 3081–3098. https://doi.org/10.1002/ejic.200300187.
(26) Oras, S.; Vlassov, S.; Vigonski, S.; Polyakov, B.; Antsov, M.; Zadin, V.; Lõhmus, R.; Mougin, K. The Effect of Heat Treatment on the Morphology and Mobility of Au Nanoparticles. *Beilstein J. Nanotechnol.* **2020**, *11*, 61–67. https://doi.org/10.3762/bjnano.11.6.
(27) Vigonski, S.; Jansson, V.; Vlassov, S.; Polyakov, B.; Baibuz, E.; Oras, S.; Aabloo, A.; Djurabekova, F.; Zadin, V. Au Nanowire Junction Breakup through Surface Atom Diffusion. *Nanotechnology* **2017**, *29* (1), 015704. https://doi.org/10.1088/1361-6528/aa9a1b.
(28) Langley, D. P.; Lagrange, M.; Giusti, G.; Jiménez, C.; Bréchet, Y.; Nguyen, N. D.; Bellet, D. Metallic Nanowire Networks: Effects of Thermal Annealing on Electrical Resistance. *Nanoscale* **2014**, *6* (22), 13535–13543. https://doi.org/10.1039/C4NR04151H.
(29) Kumar, A.; Shaikh, M. O.; Chuang, C.-H. Silver Nanowire Synthesis and Strategies for Fabricating Transparent Conducting Electrodes. *Nanomaterials* **2021**, *11* (3), 693. https://doi.org/10.3390/nano11030693.

(30) Oh, J. S.; Oh, J. S.; Shin, J. H.; Yeom, G. Y.; Kim, K. N. Nano-Welding of Ag Nanowires Using Rapid Thermal Annealing for Transparent Conductive Films. *J. Nanosci. Nanotechnol.* **2015**, *15* (11), 8647–8651. https://doi.org/10.1166/jnn.2015.11509.
(31) Li, H.; Biser, J. M.; Perkins, J. T.; Dutta, S.; Vinci, R. P.; Chan, H. M. Thermal Stability of Cu Nanowires on a Sapphire Substrate. *J. Appl. Phys.* **2008**, *103* (2), 024315. https://doi.org/10.1063/1.2837053.
(32) Vlassov, S.; Mets, M.; Polyakov, B.; Bian, J.; Dorogin, L.; Zadin, V. Abrupt Elastic-to-Plastic Transition in Pentagonal Nanowires under Bending. *Beilstein J. Nanotechnol.* **2019**, *10*, 2468–2476. https://doi.org/10.3762/bjnano.10.237.
(33) Trausa, A.; Tipaldi, C. F.; Ignatane, L.; Polyakov, B.; Oras, S.; Butanovs, E.; Vanags, E.; Smits, K. Heat-Induced Fragmentation and Adhesive Behaviour of Gold Nanowires for Surface-Enhanced Raman Scattering Substrates. *ChemEngineering* **2024**, *8* (1), 15. https://doi.org/10.3390/chemengineering8010015.
(34) Fan, M.; Andrade, G. F. S.; Brolo, A. G. A Review on the Fabrication of Substrates for Surface Enhanced Raman Spectroscopy and Their Applications in Analytical Chemistry. *Anal. Chim. Acta* **2011**, *693* (1), 7–25. https://doi.org/10.1016/j.aca.2011.03.002.
(35) Pal, P.; Bonyár, A.; Veres, M.; Himics, L.; Balázs, L.; Juhász, L.; Csarnovics, I. A Generalized Exponential Relationship between the Surface-Enhanced Raman Scattering (SERS) Efficiency of Gold/Silver Nanoisland Arrangements and Their Non-Dimensional Interparticle Distance/Particle Diameter Ratio. *Sens. Actuators Phys.* **2020**, *314*, 112225. https://doi.org/10.1016/j.sna.2020.112225.
(36) Vlassov, S.; Polyakov, B.; Dorogin, L. M.; Antsov, M.; Mets, M.; Umalas, M.; Saar, R.; Lõhmus, R.; Kink, I. Elasticity and Yield Strength of Pentagonal Silver Nanowires: In Situ Bending Tests. *Mater. Chem. Phys.* **2014**, *143* (3), 1026–1031. https://doi.org/10.1016/j.matchemphys.2013.10.042.
(37) Plimpton, S. Fast Parallel Algorithms for Short-Range Molecular Dynamics. *J. Comput. Phys.* **1995**, *117* (1), 1–19. https://doi.org/10.1006/jcph.1995.1039.
(38) Williams, P. L.; Mishin, Y.; Hamilton, J. C. An Embedded-Atom Potential for the Cu–Ag System. *Model. Simul. Mater. Sci. Eng.* **2006**, *14* (5), 817. https://doi.org/10.1088/0965-0393/14/5/002.
(39) Stukowski, A. Visualization and Analysis of Atomistic Simulation Data with OVITO–the Open Visualization Tool. *Model. Simul. Mater. Sci. Eng.* **2009**, *18* (1), 015012. https://doi.org/10.1088/0965-0393/18/1/015012.
(40) Guan, P.; Zhu, R.; Zhu, Y.; Chen, F.; Wan, T.; Xu, Z.; Joshi, R.; Han, Z.; Hu, L.; Wu, T.; Lu, Y.; Chu, D. Performance Degradation and Mitigation Strategies of Silver Nanowire Networks: A Review. *Crit. Rev. Solid State Mater. Sci.* **2022**, *47* (3), 435–459. https://doi.org/10.1080/10408436.2021.1941753.
(41) Mets, M.; Antsov, M.; Zadin, V.; Dorogin, L. M.; Aabloo, A.; Polyakov, B.; Lõhmus, R.; Vlassov, S. Structural Factor in Bending Testing of Fivefold Twinned Nanowires Revealed by Finite Element Analysis. *Phys. Scr.* **2016**, *91* (11), 115701. https://doi.org/10.1088/0031-8949/91/11/115701.
(42) Haynes, W. M. *CRC Handbook of Chemistry and Physics (95th ed.)*. https://www.taylorfrancis.com/books/mono/10.1201/b17118/crc-handbook-chemistry-physics-william-haynes (accessed 2024-01-04).
(43) Mayoral, A.; Allard, L. F.; Ferrer, D.; Esparza, R.; Jose-Yacaman, M. On the Behavior of Ag Nanowires under High Temperature: In Situ Characterization by Aberration-Corrected STEM. *J Mater Chem* **2011**, *21* (3), 893–898. https://doi.org/10.1039/C0JM02624G.
(44) Sun, S.; Kong, D.; Li, D.; Liao, X.; Liu, D.; Mao, S.; Zhang, Z.; Wang, L.; Han, X. Atomistic Mechanism of Stress-Induced Combined Slip and Diffusion in Sub-5

Nanometer-Sized Ag Nanowires. *ACS Nano* **2019**, *13* (8), 8708–8716. https://doi.org/10.1021/acsnano.9b00474.
(45) Toimil Molares, M. E.; Balogh, A. G.; Cornelius, T. W.; Neumann, R.; Trautmann, C. Fragmentation of Nanowires Driven by Rayleigh Instability. *Appl. Phys. Lett.* **2004**, *85* (22), 5337–5339. https://doi.org/10.1063/1.1826237.
(46) Kim, J.-H.; Ma, J.; Jo, S.; Lee, S.; Kim, C. S. Enhancement of Antibacterial Performance of Silver Nanowire Transparent Film by Post-Heat Treatment. *Nanomaterials* **2020**, *10* (5), 938. https://doi.org/10.3390/nano10050938.
(47) Oh, H.; Lee, J.; Lee, M. Transformation of Silver Nanowires into Nanoparticles by Rayleigh Instability: Comparison between Laser Irradiation and Heat Treatment. *Appl. Surf. Sci.* **2018**, *427*, 65–73. https://doi.org/10.1016/j.apsusc.2017.08.102.